Catalytic oxidation of the GaAs(110) surface promoted by a Cs overlayer

G. Faraci and A. R. Pennisi
Dipartimento di Fisica–Universitá di Catania, Istituto Nazionale di Fisica della Materia, Corso Italia 57, 95129 Catania, Italy

G. Margaritondo
Institut de Physique Appliquée, Ecole Polytechnique Fédérale, PH-Ecublens, CH-1015 Lausanne, Switzerland and Sincrotrone Trieste SCpA, Trieste, Italy

(Received 11 December 1995)

In order to investigate the dramatic enhancement of the oxidation rate of semiconductor materials, promoted by an alkali-metal overlayer, we exposed a GaAs(110) surface covered by a monolayer of Cs to oxygen, observing the photoemission spectra of As $2p$, Ga $2p$, Cs $4d$, and O $1s$. We show evidence that the oxidation mechanism proceeds through (i) oxygen infiltration underneath the Cs monolayer; (ii) disruption of low-binding-energy bonds Cs-As and Cs-Ga established at the Cs/GaAs(110) interface before the exposure to O_2; and (iii) oxide formation upon oxygen exposure, involving not only As and Ga but also Cs: substoichiometric and stoichiometric arsenic oxides are evident in different high-binding-energy components in the As $2p$ spectra. Ga oxide and Cs hybrid bonds were deduced by deconvolution of Ga $2p$ and Cs $4d$ core-level spectra. We show that the catalytic mechanism of the oxide promotion is due to Cs bound to the semiconducting elements through the formation of a positively charged layer which strongly attracts oxygen; afterwards, at the Cs surface, oxygen is preferentially driven toward the most stable bonds, i.e., the highest-binding-energy oxide components. [S0163-1829(96)07019-1]

INTRODUCTION

GaAs is among the semiconductors most widely used in device applications for which thin oxide layers are required. However, in normal conditions its oxidation rate is very low. The oxide layer growth on the semiconductor surface by means of oxygen exposure can be enhanced by the catalytic action of a monolayer deposition of an alkali metal.[1–4] A good example is Cs, which dramatically enhances the semiconductor oxidation rate by many orders of magnitude.[3] The mechanism of such a process is still under strong debate, since it is not clear how the metal behaves at the Cs/GaAs interface, which kind of bonds are established, and why oxygen is captured by the substrate rather than by the metal. Many studies have been devoted to the metal-semiconductor interface[5–8] and to the successive exposure of such interface to oxygen: interface studies have aimed at ascertaining which surface dangling bonds are saturated by cesium;[9] how much charge is transferred to these bonds, i.e., their ionic or covalent nature; and, most importantly, how the oxidation can proceed in the presence of low oxygen exposure. The low exposure of the interface Cs/GaAs(110) to O_2, which is the subject of the present paper, seeks to determine which one of the three elements Cs, Ga, and As involved in the oxidation is really oxidized, for instance, by direct formation of intermediate or stoichiometric oxidation states of the metal and/or of the semiconductor elements.

We show evidence that the promoted oxidation of the substrate is really due to the metal surface layer establishing weak surface bonds with the semiconductor. Consequently, the polarized surface layer strongly attracts oxygen, favoring the oxidation. The stronger binding energy of the semiconductor oxides determines the infiltration of oxygen through the Cs atoms, and the disruption of low-binding-energy bonds Cs-As and Cs-Ga. Substrate oxidation can then take place.

In order to investigate the previous questions, we performed high-resolution core-level spectra of the Cs/GaAs(110) interface exposed to O_2, as a function of the oxygen exposure. The spectra of the O $1s$, As $2p_{3/2}$, Ga $2p_{3/2}$, and Cs $4d$ levels have been analyzed in their intensity, energy position, and width. The onset of energy-shifted features and their relative intensity enabled us to identify clearly which element was involved in the oxide formation, and how these oxides evolved.

EXPERIMENT

GaAs(110) single crystals were cleaved under ultrahigh vacuum and exposed, at a pressure lower than 10^{-10} Torr and at room temperature, to Cs obtained by evaporation from a carefully outgassed SAES Getters chromate source. Photoemission spectra were obtained at the Scienta ESCA-300 (ESCA is electron spectroscopy for chemical analysis) machine of the IPA-EPFL Center of Spectromicroscopy, using an Al $K\alpha$ emission beam at 1486.7 eV. This is a high-energy resolution (better than 0.3 eV), and high-intensity photon source operating with a wide-angle double-focusing x-ray monochromator. This consists of seven crystals mounted in a hexagonal-close-packed pattern; they are heated and temperature stabilized so as to guarantee a constant photon energy. The electron analyzer is a cylindrical hemispherical analyzer coupled to a microchannel plate electron multiplier. The spectra were taken in the energy distribution mode, and the electrons detected by a hemispherical mirror analyzer as a function of the electron kinetic energy. After each Cs depo-

0163-1829/96/53(20)/13851(6)/$10.00 © 1996 The American Physical Society

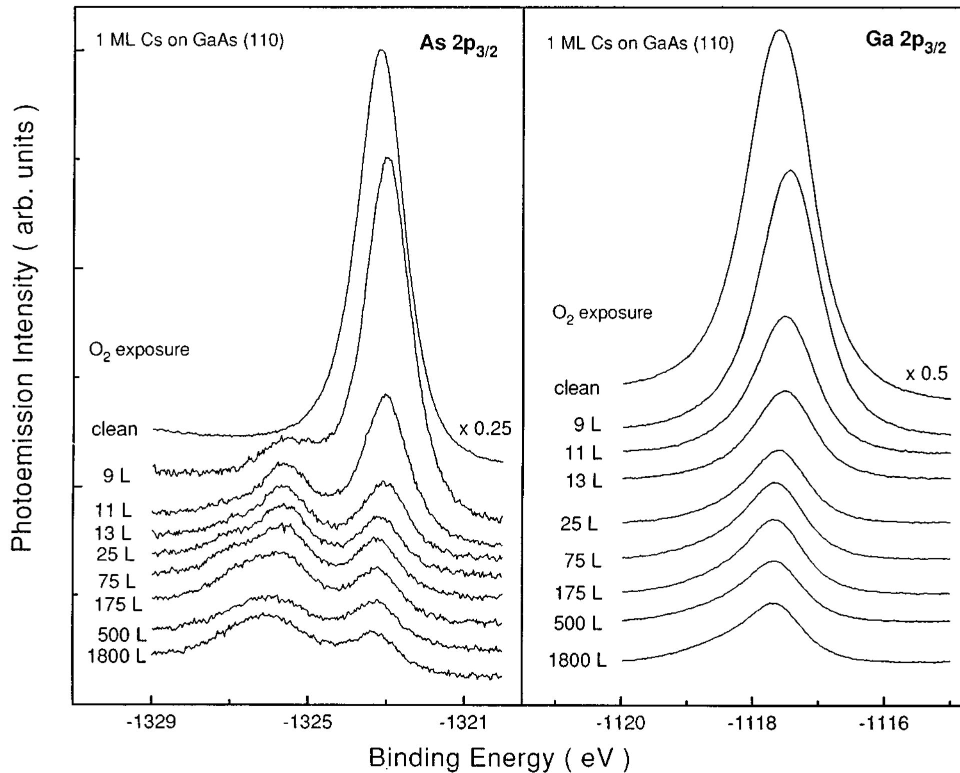

FIG. 1. Photoemission intensity of the As $2p_{3/2}$ and Ga $2p_{3/2}$ core-level spectra, for a monolayer of Cs on GaAs(110), as a function of the binding energy, at different oxygen exposures (1 L $=10^{-6}$ Torr s). The curves are normalized to the photon flux. Clearly visible, for increasing O_2 exposure, is the growth of oxide features on the high-binding-energy tail of the As $2p_{3/2}$ and the asymmetric widening of the Ga $2p_{3/2}$.

sition the surface was checked by observing the Ga $3d$, As $3d$, and Cs $3d$ and $4d$ core levels, and the valence band. Once the metal monolayer was completed, several exposures of O_2 were performed, and the evolution of the oxidation features was followed by observing the onset and the growth of higher-binding-energy features on the tail of the clean core levels. We have investigated the Ga $2p_{3/2}$, As $2p_{3/2}$, Cs $4d$, and O $1s$ core levels. For the semiconductor, deep core levels have been chosen because, at a beam energy of 1486.7 eV, the photoelectron kinetic energy guarantees a better surface sensitivity with respect to higher levels such as Ga $3d$ or As $3d$. The energy resolution of the electron analyzer was 300 meV, as derived from the Fermi edge of a clean Ag surface.

RESULTS AND DISCUSSION

For 1 ML of Cs at the interface Cs/GaAs(110), the photoemission spectra of the As $2p_{3/2}$ and Ga $2p_{3/2}$ core levels are shown in Fig. 1 for several oxygen exposures. Immediately clear is the growth of high-binding-energy features on the left tail of the As $2p_{3/2}$ spectra, whereas the Ga $2p_{3/2}$ spectra show an evident distortion of the left part of the peak. We note that the electron attenuation length corresponding to the Al $K\alpha$ photons of our source is of about 5 Å (Ref. 10) for the As $2p_{3/2}$ photoelectrons (whose kinetic energy is 163 eV), and slightly more for the Ga $2p_{3/2}$ photoelectrons (whose kinetic energy is 370.2 eV). This implies a good surface sensitivity for the substrate atoms, and an enhanced intensity for the Cs and O_2 core levels since these atoms reside only at the surface or at the interface. In Fig. 2, we show the photoemission intensity of the O $1s$ core level, and the Cs $4d$ doublet for several oxygen exposures. The broad oxygen spectrum appears composed of different overlapping contributions; a minor deformation is apparent in the Cs doublets which, however, shift with oxygen exposure. From Figs. 1 and 2 we immediately observe that the total area (intensity) of the Cs $4d$ doublets as a function of the O_2 exposure does not change at all; on the contrary, the total intensity of the As $2p_{3/2}$ and Ga $2p_{3/2}$ strongly decreases with the O_2 exposure. This implies that oxygen does cover the semiconductor, attenuating the flux of the outgoing electrons, but it does not reduce the metal spectrum. This is possible only if oxygen penetrates underneath the metal, which continues to reside on the top of the sample.

In order to distinguish the different contributions under each curve, the spectra shown in Fig. 1 were analyzed in terms of different components; the clean As $2p_{3/2}$ and Ga $2p_{3/2}$ peaks were fitted by a Doniach-Sunjic curve[11,12] convoluted to a Gaussian curve, taking into account the experimental resolution. Conversely, the high-energy features of the spectra were analyzed in terms of Gaussian components,[9,12] since they are due to intermediate (AsO_x or GaO_x) or stoichiometric (As_2O_5 or Ga_2O_3) oxide.

In Fig. 3 we compare a typical deconvolution of two semiconductor spectra at low (13 L) and high (1800 L) oxygen exposure. Besides the clean part of the core level, broad oxide components can be easily extracted. Of course, it is possible that each Gaussian oxide peak actually corresponds to several substoichiometric features, unresolved with the present resolution. In Fig. 4, a similar decomposition is shown for O $1s$ and Cs $4d$ spectra. The binding energy and relative intensity of the various features of As $2p_{3/2}$, Ga $2p_{3/2}$, Cs $4d$, and O $1s$ are reported in Tables I and II for all exposures. Note that the energy shift observed in the Cs $4d$ spectra is really due to the height modification of the (three)

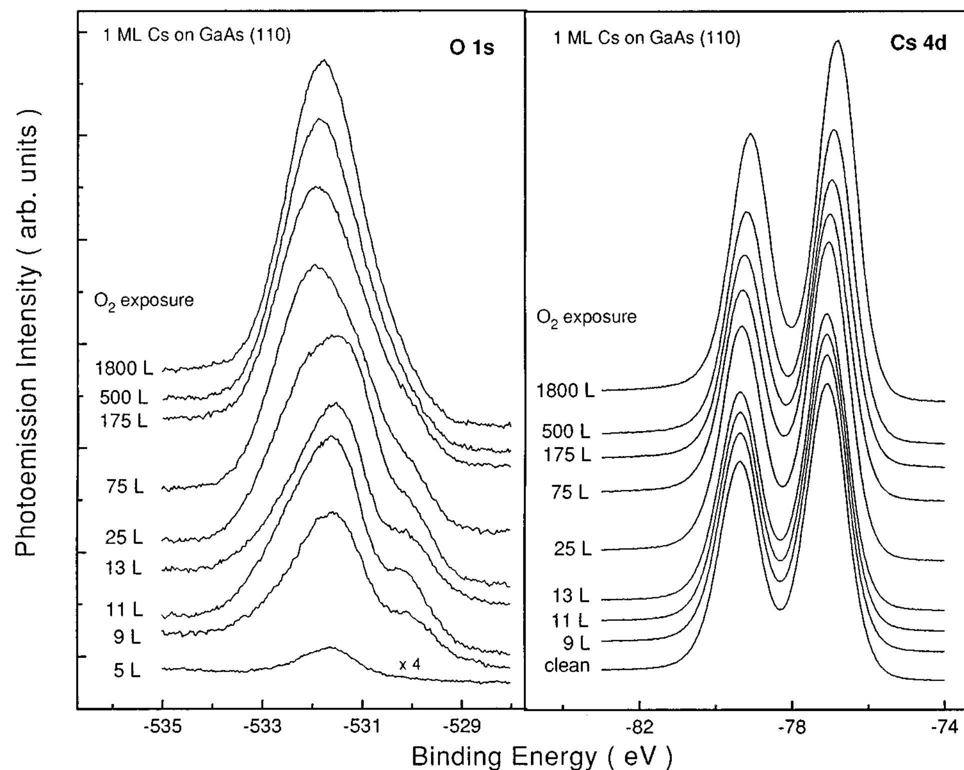

FIG. 2. Photoemission intensity of the O $1s$ and Cs $4d$ core-level spectra, for a monolayer of Cs on GaAs(110), as a function of the binding energy, at different oxygen exposures. The curves are normalized to the photon flux.

components which, however, are quite stable in energy. These components, as shown in Ref. 9, are already present in the absence of oxygen, and can then be attributed to weak bonds Cs-As ($E_1=-76.5$ eV), Cs-Ga ($E_2=-77$ eV), and Cs^+ ($E_3=-77.5$ eV) bound in ionic configuration to either As or Ga. However, from Table II we find that oxygen progressively determines a decrease of the two high-energy components of Cs $4d$ with a concomitant amplification of the third. The reduction of the Cs $4d$ high-binding-energy components clearly implies a partial disruption of the corresponding metal-semiconductor bonds. The growth of the lowest-binding-energy component, due to O_2 exposure, should now be attributed to another kind of bonding of Cs with oxygen, overlapping the previous Cs-As feature. We emphasize, however, that the metal is involved only for a minor part (less than about 10%, to 175 L, see Table II) in

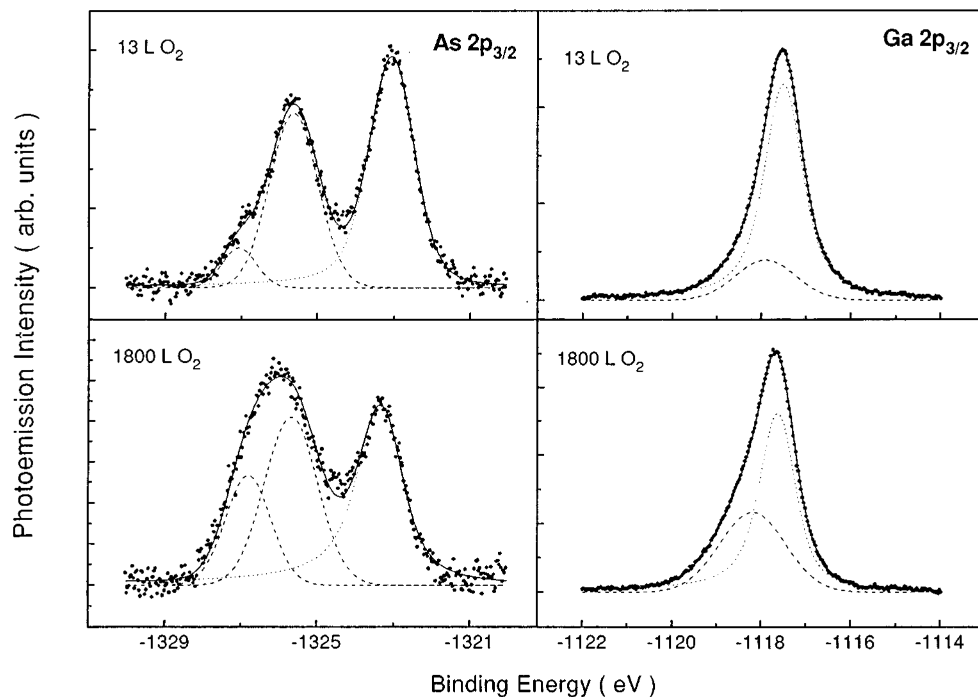

FIG. 3. Deconvolution of the As $2p_{3/2}$ and Ga $2p_{3/2}$ core-level spectra taken at two different O_2 exposures, showing the clean (dotted) and the oxide (dashed) components. The fit was performed (i) for the clean part of the spectrum by convolution of a Doniach-Sunjic curve with a Gaussian curve taking into account the experimental resolution and the thermal broadening, and (ii) for the oxide features by Gaussian curves. Note that for the As $2p_{3/2}$ two oxide components are easily resolved. The background fitted by a cubic spline was subtracted from the spectra. The solid line is the sum of the contributing curves, and closely fits the experimental points.

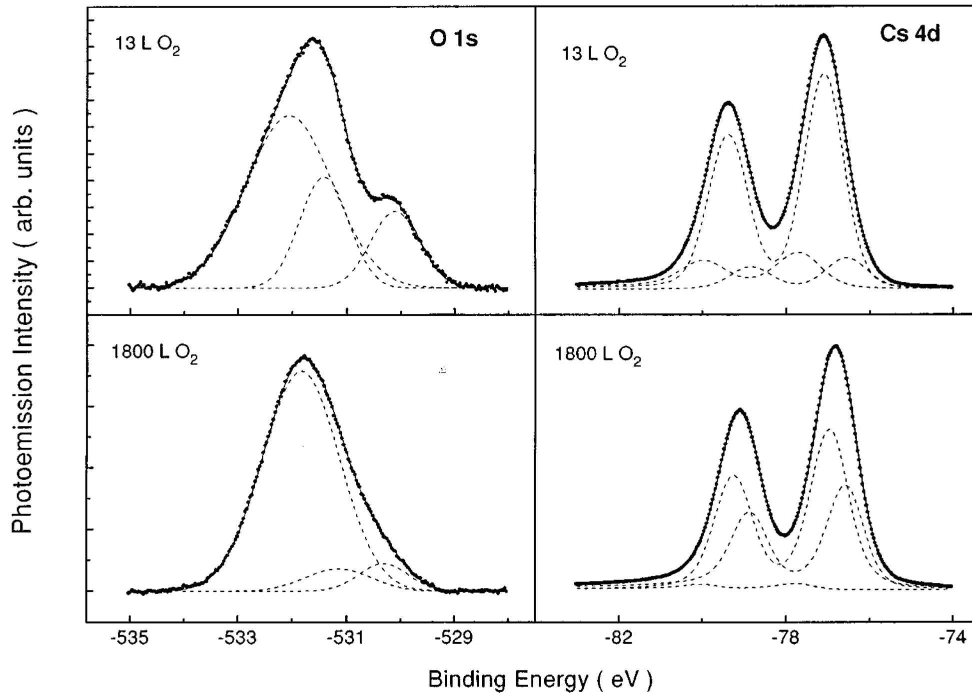

FIG. 4. Deconvolution of the O $1s$ and Cs $4d$ core-level spectra taken at two different O_2 exposures. For the oxygen spectra, Gaussian curves were used; for the Cs doublets, we adopted spin-orbit energy split and mutually shifted Doniach-Sunjic curves, convolved with a Gaussian curve taking into account the experimental resolution and the thermal broadening. The background fitted by a cubic spline was subtracted from the spectra. The solid line is the sum of the contributing curves, and closely fits the experimental points.

these oxygen-induced modifications of its configuration. Then a possible scenario could be the formation of additional hybrid bonds where oxygen bridges a metal atom with a semiconductor element in a configuration Cs-O-O-X (X=As, Ga) or Cs-O-X. This point will be discussed further in connection to the O $1s$ analysis. In any case, we can exclude[13] the presence of cesium peroxide, or superoxide, since only minor effects modify the Cs spectra with respect to the dramatic oxide enhancement of the As $2p_{3/2}$ and Ga $2p_{3/2}$.

In fact, although the total intensity of the As $2p_{3/2}$ and Ga $2p_{3/2}$ decay with O_2 exposure, the part of the spectra due to oxide features shows an increasing relative intensity, as seen in Fig. 5. Here the oxide areas rapidly increase around 10 L, with a trend very similar to the O $1s$ photoemission intensity, shown in the same figure. After 100 L the curves tend to saturate. From these remarks we conclude that the oxidation takes place under the metal mainly involving As and Ga.

The interpretation of the present measurements confirms the important role of the metal in the catalytic oxidation of the substrate. Measurements of the oxidation of GaAs(110) without a Cs overlayer (not shown here) indicate that no oxidation is visible at least up to 10^5 L. The Cs metal overlayer then acts as a capture layer for oxygen, since its deposition in the absence of oxygen determines a positive polarized surface because of ionic bonds with the substrate. However, these preexisting bonds are quite weak and unstable in comparison to the higher binding energy of the bonds that can be formed by oxygen with the semiconducting elements (see Tables I and II). In other terms As and Ga are in a much more stable configuration if bound to oxygen than when bound to Cs. This energy requirement justifies the disruption of Cs-As and Cs-Ga bonds and the formation of

TABLE I. Energy position and relative intensity of the components obtained from the best fit of the As $2p_{3/2}$ and Ga $2p_{3/2}$ core-level spectra, at the specified oxygen exposure (1 L=10^{-6} Torr s). The uncertainty for the energies is less than ±0.1 eV, for intensities less than ±2%. In both cases, the first component is the clean feature, the other(s) the oxide component(s).

	As $2p_{3/2}$						Ga $2p_{3/2}$			
O_2 exposure	E_1 (eV)	E_2 (eV)	E_3 (eV)	I_1 %	I_2 %	I_3 %	E_1 (eV)	E_2 (eV)	I_1 %	I_2 %
5 L	−1323.1			100			−1117.6	−1118.3	98	2
9 L	−1323.0	−1325.4		90	10		−1117.4	−1118.3	96	4
11 L	−1323.0	−1325.6	−1327.2	70	27	3	−1117.5	−1118.1	91	9
13 L	−1323.0	−1325.6	−1327.1	55	39	6	−1117.6	−1117.9	81	19
25 L	−1323.1	−1325.6	−1327.1	50	39	11	−1117.6	−1118.0	74	26
75 L	−1323.2	−1325.6	−1327.1	44	39	17	−1117.6	−1118.1	74	26
175 L	−1323.2	−1325.6	−1327.0	44	39	17	−1117.6	−1118.1	66	34
500 L	−1323.3	−1325.6	−1326.8	51	33	16	−1117.6	−1118.2	66	34
1800 L	−1323.3	−1325.7	−1326.8	44	36	20	−1117.6	−1118.2	61	39

TABLE II. Energy position and relative intensity of the components obtained from the best fit of the Cs 4d and O 1s core-level spectra, at the specified oxygen exposure (1 L $=10^{-6}$ Torr s). The uncertainty for the energies is less than ± 0.1 eV, for intensities less than $\pm 2\%$.

	Cs 4d						O 1s					
O_2 exposure	E_1 (eV)	E_2 (eV)	E_3 (eV)	I_1 %	I_2 %	I_3 %	E_1 (eV)	E_2 (eV)	E_3 (eV)	I_1 %	I_2 %	I_3 %
0 L	−76.5	−77.1	−77.6	11	73	16						
1 L	−76.5	−77.0	−77.6	12	72	16	−531.8	−531.5		6	94	
5 L	−76.5	−77.0	−77.5	14	71	15	−532.2	−531.6	−530.1	19	76	5
9 L	−76.5	−77.0	−77.5	15	69	16	−532.2	−531.5	−530.0	40	45	15
11 L	−76.4	−77.0	−77.5	12	74	14	−532.0	−531.4	−530.0	57	28	15
13 L	−76.5	−77.1	−77.6	11	73	16	−532.1	−531.4	−530.1	61	23	16
25 L	−76.4	−77.0	−77.5	17	75	8	−531.9	−531.1	−530.0	80	11	9
75 L	−76.5	−77.0	−77.7	11	81	8	−531.9	−530.9	−530.0	84	7	9
175 L	−76.4	−77.0	−77.7	14	80	6	−531.9	−530.7	−530.0	84	12	4
500 L	−76.5	−77.0	−77.7	29	67	4	−531.9	−530.7	−530.1	87	9	4
1800 L	−76.6	−77.0	−77.7	39	58	3	−531.9	−530.8	−530.2	90	6	4

the oxides. This is confirmed by the modifications found on the Cs 4d spectra where the decrease of the higher-energy components has been attributed to this disruption.

Finally, we discuss the oxygen features, reported in Table II; here too, three broad features can be extracted which can be compared to those reported by Qiu *et al.* in Ref. 13. Although this study concerns the reaction of Cs with molecular O_2 at low temperature, we can compare our components to those reported by these authors in their Fig. 5. As expected, in our data we do not find any structure at -540 eV; i.e., no physisorbed unbound O_2 was detected. In addition, superoxide species at -535 eV are not present; on the contrary, we find three components, due to bound oxygen, which can be distinguished according to the residual charge remaining on the oxygen atom: the highest binding energy at about -532 eV is due to $O_2{}^{2-}$, i.e., to oxygen in single or mixed bonding (e.g., Cs-O-O-As, etc.).[14] The other two components can be attributed to atomic oxygen O^{2-} directly bound to the semiconductor elements in stoichiometric or intermediate oxidation state. At low exposure, the atomic configuration is privileged because of the high reactivity of the clean interface, visible in the fast rise of the oxide intensity around 10 L, shown in Fig. 5. At high exposure, as the total amount of oxygen is increased, the molecular configuration increases relatively, probably because more and more mixed bonds are involved.

A quantitative determination of which absolute percentage of metal or semiconductors is involved in the oxidation process is, however, quite difficult, since the cross section of each oxidation state usually changes with respect to the pure crystalline state. Furthermore, the plots of Fig. 5 demonstrate that the dynamical chemisorption of oxygen, after the initial fast rise, proceeds at a very slow rate because of the surface charge saturation.

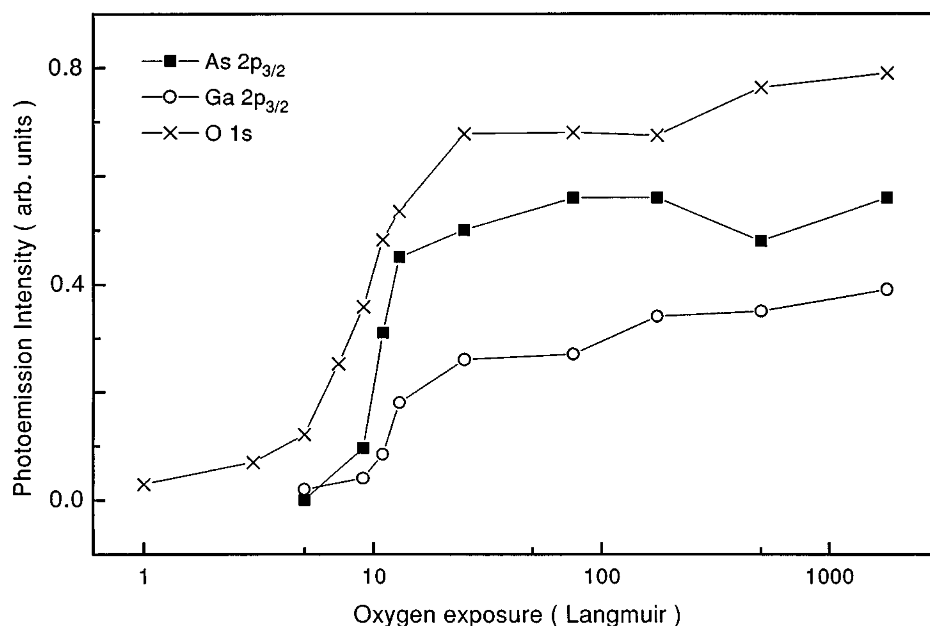

FIG. 5. Total photoemission intensity, normalized to the photon flux vs oxygen exposure of the O 1s spectrum, where the plot shows how much oxygen is indeed adsorbed at the Cs/GaAs(110) interface; As $2p_{3/2}$ oxide features, with respect to the total area of the core level; and the Ga $2p_{3/2}$ oxide feature, with respect to the total area of the core level. The lines are a guide to the eye.

In conclusion, the present measurements have clarified the catalytic oxidation mechanism by which a cesium monolayer deposited on GaAs(110) enhances the oxidation rate of the substrate by many orders of magnitude. It involves, in comparable amounts, both As and Ga.

ACKNOWLEDGMENTS

This work was supported by the Istituto Nazionale di Fisica della Materia, by the Fond National Suisse de la Recherche Scientifique, and by the Ecole Polytechnique Fédérale de Lausanne.

[1] T. Kendelewicz, P. Soukiassian, M. H. Bakshi, Z. Hurych, I. Lindau, and W. E. Spicer, Phys. Rev. B **38**, 7568 (1988).

[2] W. E. Spicer, I. Lindau, C. Y. Su, P. W. Chye, and P. Pianetta, Appl. Phys. Lett. **33**, 934 (1978).

[3] G. Hughes and R. Ludeke, J. Vac. Sci. Technol. B **4**, 1109 (1986).

[4] H. I. Starnberg, P. Soukiassian, M. H. Bakshi, and Z. Hurych, Phys. Rev. B **37**, 1315 (1988).

[5] L. J. Whitman, Joseph A. Stroscio, R. A. Dragoset, and R. J. Celotta, Phys. Rev. Lett. **66**, 1338 (1991).

[6] J. Ortega, R. Pérez, F. J. García-Vidal, and F. Flores, Appl. Surf. Sci. **56**, 264 (1992); J. E. Ortega and R. Miranda, *ibid.* **56**, 211 (1992).

[7] J. Hebenstreit, M. Heinemann, and M. Scheffler, Phys. Rev. Lett. **67**, 1031 (1991).

[8] B. Reihl, R. Dudde, L. S. O. Johansson, K. O. Magnusson, S. L. Sorensen, and S. Wiklund, Appl. Surf. Sci. **56**, 123 (1992).

[9] G. Faraci, A. R. Pennisi, F. Gozzo, S. La Rosa, and G. Margaritondo, Phys. Rev. B **53**, 3987 (1996).

[10] D. A. Shirley, in *Photoemission in Solids I*, edited by M. Cardona and L. Ley (Springer-Verlag, Berlin, 1978), p. 193.

[11] S. Doniach and M. Sunjic, J. Phys. C **3**, 285, 1970; G. K. Wertheim, D. M. Riffe, and P. H. Citrin, Phys. Rev. B **45**, 8703 (1992).

[12] G. Faraci, S. La Rosa, A. R. Pennisi, Y. Hwu, and G. Margaritondo, J. Appl. Phys. **78**, 4091 (1995).

[13] S. L. Qui, C. L. Lin, J. Chen, and Myron Strongin, Phys. Rev. B **41**, 7467 (1990).

[14] B. Woratschek, W. Sesselmann, J. Küppers, and G. Ertl, J. Chem. Phys. **86**, 2411 (1987).